HOKKAIDO UNIVERSITY

Title	H2O2-induced Greenhouse Warming on Oxidized Early Mars
Author(s)	Ito, Yuichi; Hashimoto, George L.; Takahashi, Yoshiyuki O. et al.
Citation	Astrophysical journal, 893(2), 168 https://doi.org/10.3847/1538-4357/ab7db4
Issue Date	2020-04-20
Doc URL	https://hdl.handle.net/2115/81090
Rights	This is the Accepted Manuscript version of an article accepted for publication in Astrophysical journal. IOP Publishing Ltd is not responsible for any errors or omissions in this version of the manuscript or any version derived from it. The Version of Record is available online at https://iopscience.iop.org/article/10.3847/1538-4357/ab7db4.
Rights(URL)	https://creativecommons.org/licenses/by-nc-nd/4.0/
Type	journal article
File Information	Astrophys. J.893-2_168.pdf

Hokkaido University Collection of Scholarly and Academic Papers : HUSCAP

1

Draft version January 2, 2020
Typeset using LaTeX **twocolumn** style in AASTeX63

H_2O_2 induced greenhouse warming on oxidized early Mars

Yuichi Ito [1,2] George L. Hashimoto [3] Yoshiyuki O. Takahashi [4] Masaki Ishiwatari [2] and Kiyoshi Kuramoto [2]

[1] *Department of Physics and Astronomy, University College London, London WC1E 6BT, United Kingdom*
[2] *Department of Cosmosciences, Hokkaido University, Sapporo 060-0810, Japan*
[3] *Department of Earth Sciences, Okayama University, Okayama 700-8530, Japan*
[4] *Department of Planetology, Kobe University, Kobe 657-8501, Japan*

Submitted to ApJ

ABSTRACT

The existence of liquid water within an oxidized environment on early Mars has been inferred by the Mn-rich rocks found during recent explorations on Mars. The oxidized atmosphere implied by the Mn-rich rocks would basically be comprised of CO_2 and H_2O without any reduced greenhouse gases such as H_2 and CH_4. So far, however, it has been thought that early Mars could not have been warm enough to sustain water in liquid form without the presence of reduced greenhouse gases. Here, we propose that H_2O_2 could have been the gas responsible for warming the surface of the oxidized early Mars. Our one-dimensional atmospheric model shows that only 1 ppm of H_2O_2 is enough to warm the planetary surface because of its strong absorption at far-infrared wavelengths, in which the surface temperature could have reached over 273 K for a CO_2 atmosphere with a pressure of 3 bar. A wet and oxidized atmosphere is expected to maintain sufficient quantities of H_2O_2 gas in its upper atmosphere due to its rapid photochemical production in slow condensation conditions. Our results demonstrate that a warm and wet environment could have been maintained on an oxidized early Mars, thereby suggesting that there may be connections between its ancient atmospheric redox state and possible aqueous environment.

Keywords: planets and satellites: atmospheres — planets and satellites: terrestrial planets

1. INTRODUCTION

One of the most intriguing and debatable problems in planetary science is elucidating how an early Martian surface environment could have been warm enough to sustain liquid water (Wordsworth 2016; Ramirez & Craddock 2018). Climate models have shown that a CO_2–H_2O atmosphere alone could not have kept early Mars warm enough to sustain liquid water globally even if any amount of atmospheric pressure is assumed (e.g., Kasting 1991). This suggests that the other greenhouse components could have played a key role in the early Martian atmosphere. Current theoretical models suggest that the warming of early Mars was caused by a CO_2–H_2O atmosphere combined with additional greenhouse substances; clouds (e.g., Forget & Pierrehumbert 1997; Wordsworth et al. 2013); reducing gases such as H_2, CH_4, and NH_3 (e.g., Ramirez et al. 2014; Ramirez 2017; Wordsworth et al. 2017; Sagan & Mullen 1972; Kasting et al. 1992); and/or volcanic gases such as H_2S and SO_2 (e.g., Postawko & Kuhn 1986; Johnson et al. 2008; Tian et al. 2010).

Recently, *NASA*'s Curiosity rover discovered a high abundance of Mn in sedimentary rocks (Lanza et al. 2016). During the era in which the observed Mn-oxide-rich rocks at Gale crater would have precipitated out, Mars may have had both liquid water on its surface and a highly oxidized atmosphere (Lanza et al. 2016; Noda et al. 2019). Furthermore, the existence of rocks with a high concentration of manganese at Endeavour

[1] January 2, 2020
Corresponding author: Yuichi Ito
yuichi.ito.kkyr@gmail.com

crater (Arvidson et al. 2016) suggests that such an oxidized and wet surface environment was a global phenomenon at that time. These findings suggest that the early Martian surface had once experienced a wet and warm environment, but with the absence of reduced gas species that would have enhanced the greenhouse effect of a CO_2–H_2O dominated Martian atmosphere to allow the existence of liquid water. One might consider SO_2 as a candidate greenhouse gas in an oxidized atmosphere (e.g., Johnson et al. 2008), but its presence seems unlikely during this era because Mn and S are not correlated in the rocks found at Gale crater (Lanza et al. 2016).

In an attempt to address this uncertainty, in this study we investigate the greenhouse effect due to hydrogen peroxide (H_2O_2) gas in the early Martian atmosphere. Previously, it had been proposed that H_2O_2 gas was responsible for oxidizing the early Martian surface (e.g., Zahnle et al. 2008). Although the idea that H_2O_2 was one of the greenhouse gases responsible for the warming of early Mars has widely been ignored, H_2O_2 does absorb radiation at wavenumbers near 500 cm^{-1}, where the blackbody radiation at a temperature of 250 K has peak intensity and CO_2 has an absorption window, as shown in Fig. 1 (see also Figure 4 in Wordsworth 2016). Also, the absorption cross section of H_2O_2 is larger than those of known greenhouse gases such as SO_2, NH_3, CH_4 and OCS in a wavenumber range from 250 cm^{-1} to 450 cm^{-1}, as shown in Fig. 2.

The remainder of this paper is organized as follows. In Section 2, we describe our atmospheric model and numerical setup. In Section 3 we show the surface temperature as a function of H_2O_2 abundance under the conditions that may have been present on early Mars. We discuss the photochemical production and condensation of H_2O_2 in a warm and wet early Martian atmosphere and the possible warming scenario of H_2O_2 in an oxidized early Martian environment in Section 4. Finally we summarize our results in Section 5.

2. ATMOSPHERIC MODEL

We set up a vertical, one-dimensional CO_2-dominant atmospheric model and determine the surface temperature required to achieve balance between the absorbed solar radiation and the outgoing planetary radiation with approximated radiative–convective equilibrium temperature-pressure profiles and given compositions. The numerical scheme is based on the same line-by-line calculations used in the calculations of the surface temperature warmed by H_2O (Schaefer et al. 2016) and CO_2–H_2–CH_4 atmospheres (Wordsworth et al. 2017).

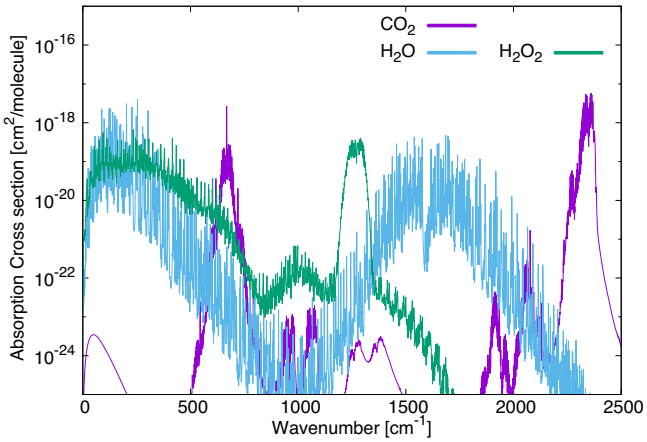


Figure 1. Absorption cross sections of three oxidized gases, CO_2 (magenta), H_2O (cyan), and H_2O_2 (green) at 250 K and 1 bar, as functions of wavenumber. These cross sections are produced using the line profile calculation code EXOCROSS (Yurchenko et al. 2018). The absorption data and the assumed line profiles are described in Sec. 2.

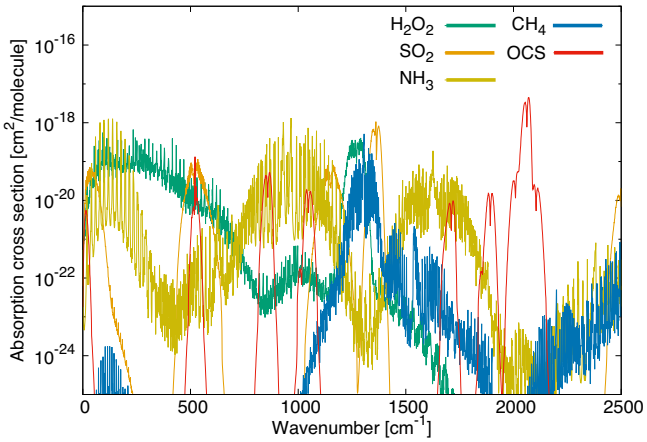


Figure 2. Absorption cross sections of H_2O_2 (green) and four greenhouse gases, SO_2 (orange), NH_3 (yellow), CH_4 (blue) and OCS (red) at 250 K and 1 bar, as functions of wavenumber. These cross sections are calculated using EXOCROSS (Yurchenko et al. 2018) and HITRAN2012 (Rothman et al. 2013), assuming a Voigt profile truncated at 25 cm^{-1} from the line center.

The atmosphere in hydrostatic equilibrium is vertically divided into 100 layers from the ground to the top of the atmosphere (1×10^{-4} bar for the model atmosphere). The surface pressure ranges from 0.01–3 bar. The vertical grid of the atmosphere is set so that the logarithms of pressure are evenly spaced. Following previous models (Ramirez et al. 2014; Ramirez 2017), we set the modeled atmosphere to one composed of 95% CO_2, fully-saturated H_2O, fully-saturated or different

mixing ratios of H_2O_2, and ≤ 5 % N_2. For the saturated H_2O_2 amount, we calculate the vapor pressure using the Clausius-Clapeyron equation. Then, we use the thermal properties of H_2O_2 (Foley & Giguére 1951a) and its saturation vapor pressure of 4.69×10^{-4} bar at the melting point (272.69 K) as a reference pressure (Manatt & Manatt 2004). In the other cases, the molar fraction of H_2O_2 is assumed to be vertically constant and its value was in the range from 10 ppb to 10 ppm. Additionaly, the abundance of H_2O is determined by the saturation vapor pressure of water (Eqs. 11 and 12 in Kasting et al. 1984).

The atmospheric temperature profile is assumed to be that of a moist adiabat of H_2O and CO_2 from the surface to the tropopause and an isothermal stratosphere above the tropopause. Using the heat capacity, c_p, given by the Shomate equation[1], the vapor amount and latent heat of H_2O (Eq.12 in Kasting et al. 1984) and the gravity of Mars, g, the moist adiabat of H_2O is given by Eq. (2.48) in Andrews (2000). Decreasing gravity with altitude is included in this model. The moist adiabat of CO_2 is adopted where the moist adiabat of H_2O is colder than the saturation vapor pressure of CO_2 using Eqs. A5 and A6 in Kasting (1991). We assume that the stratospheric temperature is 155 K (~ 167 K$\times 0.75^{1/4}$), which is based on the results of Kasting (1991), who uses 167 K as the stratospheric temperature for current solar heating and scales it for different solar heating rates by assuming that the stratospheric temperature is proportional to the skin temperature.

Using the atmospheric structure described above, we calculate the outgoing planetary radiation based on a line-by-line radiative transfer calculation. The outgoing planetary radiation is given by

$$F_p = 2\pi \int B_\nu(T_{\rm surf}) \int_0^1 \mu e^{-\tau_{\nu,{\rm surf}}/\mu} d\mu d\nu + 2\pi \int \int_0^{\tau_{\nu,{\rm surf}}} \int_0^1 B_\nu(t_\nu) e^{-\tau_\nu/\mu} d\mu d\tau_\nu d\nu, \quad (1)$$

where $T_{\rm surf}$ is the surface temperature, μ is the cosine of the zenith angle, B_ν is the Planck function at wavenumber, ν, and $\tau_{\nu,{\rm surf}}$ is the total optical depth of the atmosphere. In hydrostatic equilibrium, the optical depth is given by

$$\frac{d\tau_\nu}{dP} = \frac{\sum \chi_A \sigma_{\nu,A}}{\bar{m} g}, \quad (2)$$

where P is atmospheric pressure, $\bar{m}$ is the mean mass of the atmospheric gas particles, and χ_A and $\sigma_{\nu,A}$ are the molar fraction and absorption cross section of an absorber A, respectively. Following Ramirez (2017) and Kopparapu et al. (2013), the line absorption cross section profile of CO_2 is assumed to be a sub-Lorentzian (Perrin & Hartmann 1989) truncated at 500 cm^{-1} from the line center, while that of H_2O is assumed to be a Voigt profile truncated at 25 cm^{-1} from the line center. The line profile of H_2O_2 is also assumed to be a Voigt profile truncated at 25 cm^{-1} from the line center. For the line absorption of each gas species, the line data given by HITRAN2012 (Rothman et al. 2013) and the line profile calculation code EXOCROSS (Yurchenko et al. 2018) are used in this model. Additionally, the collision-induced absorption of CO_2–CO_2 (Gruszka & Borysow 1997; Baranov et al. 2004) is considered. In practice, to save memory and CPU time, we have prepared a numerical table in which the absorption cross sections are given as functions of temperature, T, and $\log_{10} P$. The table was created using values of $T = 150, 200, 250, 300$ and 350 K, and $\log_{10}$ (P/bar)$= -4, -3, -2, -1, 0$ and 1. We evaluate the integral shown in Eq. (1) over a wavenumber range from 1 cm^{-1} to 10000 cm^{-1} with a resolution of 1 cm^{-1}. The numerical integration of Eq. (1) with respect to the zenith angle is performed using the exponential integral calculation code presented by Press et al. (1996), while the other integrals are evaluated using trapezoidal integration.

We iteratively determine the surface temperature at which the outgoing planetary radiation balances the absorbed solar radiation. The absorbed solar radiation is given by $(1 - A_p)F_{\rm sol}/4$, where A_p is the planetary albedo and $F_{\rm sol}$ is the solar flux. The solar flux is assumed to be $F_{\rm sol} = 590 \times 0.75$ W/m^2, and we use the planetary albedo of a wet CO_2(95%)-N_2(5%) atmosphere not warmed by any additional greenhouse mechanism (Ramirez et al. 2014, private communication). Note that our assumed planetary albedo underestimates the surface temperature in a warm atmosphere with enhanced saturated–H_2O content more than the atmosphere not warmed by H_2O_2. This is because the absorption of solar radiation by H_2O decreases the planetary albedo (Kasting 1988), and H_2O_2 might work in the same way. While the Rayleigh scattering cross section per a H_2O_2 molecule is comparable with that of CO_2 based on its electric dipole polarizability (Maroulis 1992), the abundance of H_2O_2 in our model is too low (up to 10 ppm) to increase the planetary albedo. Also, though there is no public absorption data of H_2O_2 in the optical regime (see Fig.3 of Tennyson & Yurchenko 2018), its absorption in the optical is likely to not be

[1] http://old.vscht.cz/fch/cz/pomucky/fchab/Shomate.html

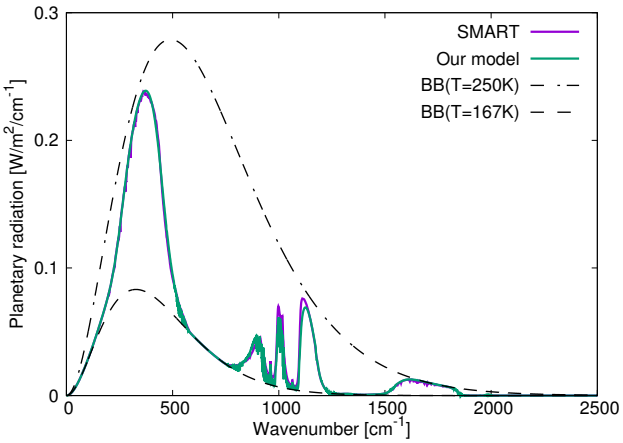


Figure 3. Outgoing planetary radiation as a function of wavenumber for a dry, 2 bar CO_2 atmosphere, comparing the result calculated by our line-by-line model (green) against the result produced with the SMARTS code (violet). In each model, a dry CO_2(95%)-N_2(5%) atmosphere with a pressure of 2 bar, a surface temperature of 250 K and a stratospheric temperature of 167 K is assumed. Also, the assumed temperature profile follows the dry and moist adiabatic lapse rate of CO_2. The plotted SMART data are the same with those shown in Figure S2 of Ramirez et al. (2014) (Ramses Ramirez, private communication). The black dashed curves show blackbody radiation, of which the temperatures are indicated by BB(T).

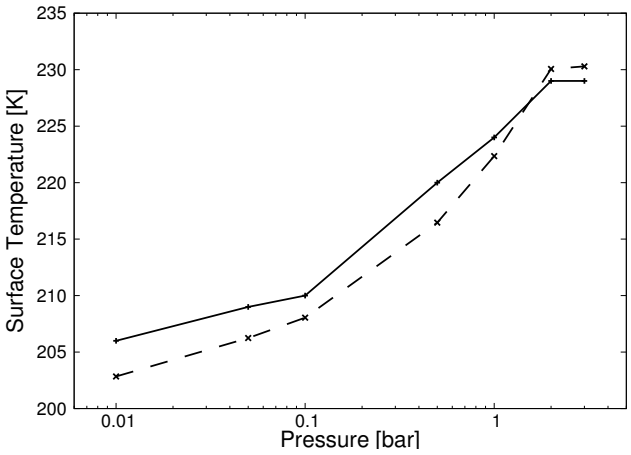


Figure 4. Surface temperature as a function of surface pressure for wet CO_2(95%)-N_2(5%) atmospheres, comparing the result calculated by our model (solid) against the result of Ramirez et al. (2014) (dotted).

very strong (see the MPI–Mainz UV/VIS Spectral Atlas[2]; Keller-Rudek et al. 2013).

[2] http://satellite.mpic.de/spectral_atlas/index.html

2.1. *MODEL VALIDATION*

We have performed two benchmark tests of our simulation code, and we have confirmed that our model reproduce the numerical solutions for the dry and wet CO_2-rich atmospheres of early Mars shown in Ramirez et al. (2014).

We first compare our line-by-line model against a well-tested line-by-line model, SMART (Meadows & Crisp 1996), for a dry, 2-bar CO_2(95%)-N_2(5%) atmosphere. With the same temperature profile shown in Figure S1 of Ramirez et al. (2014), we calculated the outgoing planetary radiation using our model. Fig. 3 shows a comparison between the SMART result and that from our model. Our model spectra agree well with the SMART spectra, although there is some difference in the wavenumber region from 800 cm^{-1} to 1200 cm^{-1}, which is likely due to the different absorption data used in both studies. The total flux of our model is 87.2 W/m^2, which agrees well with that found by SMART (88.4 W/m^2). Note that the calculated fluxes differ by at most 0.05 %, even if we double the resolution of the wavenumber or the number of vertical layers.

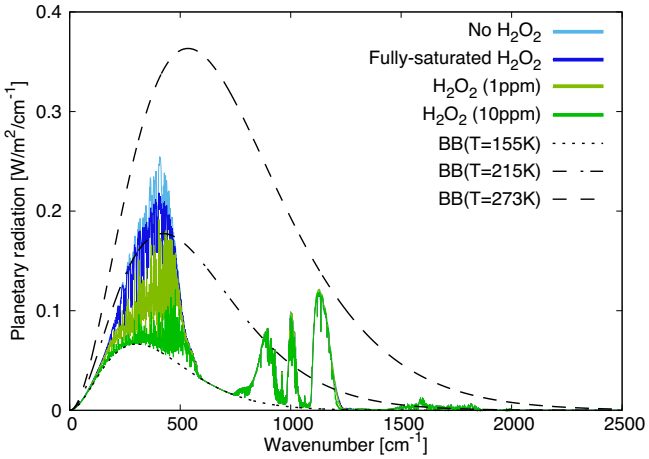
Next, we compare the surface temperatures of a wet, 2-bar CO_2(95%)-N_2(5%) atmosphere with that calculated by the one-dimensional radiative convective model Ramirez et al. (2014). Our results agrees well with those of Ramirez et al. (2014), as shown in Fig. 4, where the differences in the calculated surface temperatures are no more than 4 K. Because the results of our models agree to within 2 % of the previous studies, we have confirmed that our model is consistent with these models.

3. RESULTS

Fig. 5 (a) shows the outgoing planetary radiation for a fixed surface pressure and temperature of 2 bar and 273 K, respectively. When the atmosphere consists of H_2O and CO_2 (cyan), there are atmospheric windows at wavenumbers below 500 cm^{-1} and around 1000 cm^{-1}, which are consistent with the results of previous climate models (e.g., Wordsworth 2016; Ramirez 2017). The addition of H_2O_2 reduces the planetary radiation at wavenumbers below 500 cm^{-1} due to its strong far–IR absorption (blue, olive, green). Although H_2O_2 effectively absorbs photons with wavenumbers around 1200 cm^{-1}(Fig. 1), this only slightly affects the outgoing planetary radiation because CO_2 also absorbs photons at the same wavenumbers.

The outgoing planetary radiation is 87.6 W/m^2 for an H_2O_2 free atmosphere (cyan), which decreases drastically when H_2O_2 is added. For vertically constant molar fractions of 1 ppm (olive) and 10 ppm (green) of H_2O_2, the outgoing planetary radiation is 68.8 W/m^2

(*a*) Outgoing planetary radiation



(*b*) Atmospheric structure

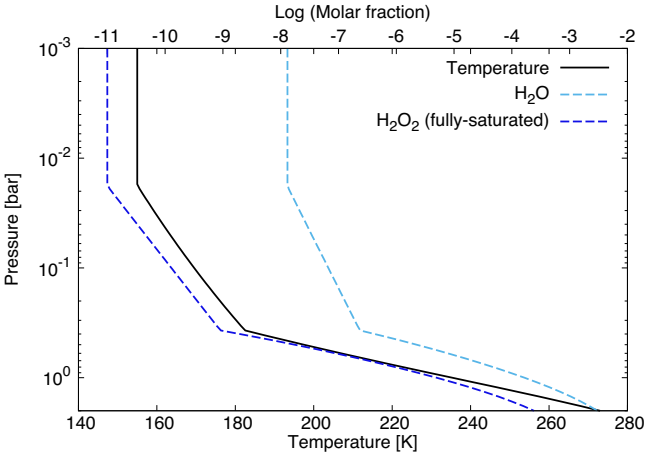


Figure 5. Impact of H_2O_2 on the outgoing planetary radiation for a surface pressure of 2 bar and a surface temperature of 273 K. *Panel (a)* — the outgoing planetary radiation as a function of wavenumber for the atmospheres without H_2O_2 and with different amounts of H_2O_2. The black dashed curves show the blackbody radiation, the temperatures of which are indicated, BB(T). *Panel (b)* —the temperature-pressure profile and the vertical distributions of H_2O and saturated H_2O_2 in the atmosphere.

and 56.5 W/m^2, respectively. If the abundance of H_2O_2 can be constrained by the saturation vapor pressure, the planetary radiation is 84.2 W/m^2 (blue), and the greenhouse effect of H_2O_2 is not remarkable. This is because the abundance of saturated H_2O_2 is too low in the low pressure region to absorb photons effectively (Fig. 5 (b)).

Next, Fig.6 shows the surface temperature as a function of surface pressure. The differences in surface temperatures between the atmospheres without H_2O_2 (black) and with saturated H_2O_2 (blue) are at most 4 K. However, in the case of abundant H_2O_2, the planetary surface is warm enough to sustain liquid water

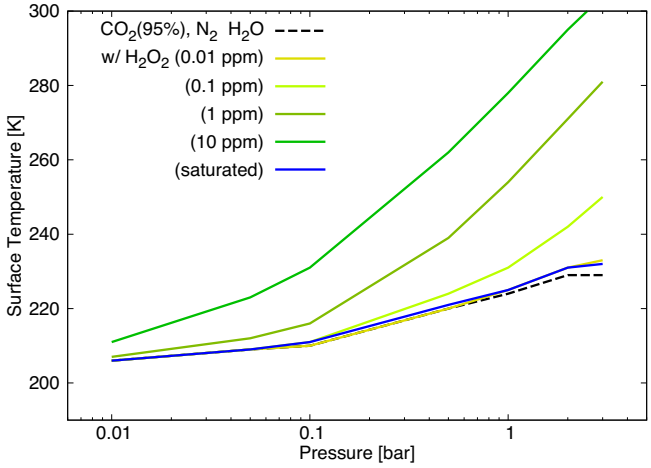


Figure 6. Surface temperature as a function of surface pressure. The dashed curve represents the atmosphere without H_2O_2while the solid curves show the atmospheres containing a saturated amount and vertically constant molar fractions of H_2O_2. Note that, the case of 0.01 ppm of H_2O_2 (yellow) is almost identical to those of saturated- (blue) and free-H_2O_2 (black).

(Fig.6). In particular, for the 2 bar atmosphere with added 1 ppm (olive) or 10 ppm (green) of H_2O_2, the surface temperature increases by about 40 K or 65 K from that of the H_2O_2-free case ($\sim$ 230 K), respectively. Our results show that a concentration of only 1 ppm level of H_2O_2 is sufficient to effectively cut off the outgoing planetary radiation and warm the planetary surface to temperatures above 273 K.

4. DISCUSSION

4.1. *H_2O_2 in a wet and oxidized atmosphere*

H_2O_2 is much more abundant in a wet and oxidized atmosphere, though the concentration of H_2O_2 in the current dry Martian atmosphere is about 10 ppb (Encrenaz et al. 2004). Although chemical models suggest that the concentration of H_2O_2 reaches at most 0.1 ppm in dry atmospheres (Parkinson & Hunten 1972; Gao et al. 2015), a wet and oxidized atmosphere which is suitable for the formation of H_2O_2 would contain H_2O_2 in a concentration higher than 0.1 ppm. This is because H_2O_2 is produced through the chemical reactions of HO_x gas species such as H, OH and HO_2 which originate from H_2O. Also, the abundance of H_2O_2 would be higher in an oxidized atmosphere because such an atmosphere inhibits the regeneration of H_2O from HO_x and enhances the production of H_2O_2.

In a wet and oxidized Martian atmosphere, the photolysis of H_2O_2 is considered to be an effective pathway to regenerate CO_2 (Yung & Demore 1999). This regen-

eration is necessary because CO_2 is destroyed by far-UV irradiation ($\lambda \leq$227.5 nm) from the Sun via;

$$CO_2 + h\nu \rightarrow CO + O. \quad \text{(R1)}$$

Indeed CO_2 regeneration is required to maintain the CO_2 atmosphere over geological timescales. In a wet atmosphere, H_2O_2 can be sufficiently produced as an intermediate product through the following catalytic cycle:

$$2(H + O_2 + M \rightarrow HO_2 + M), \quad \text{(R2)}$$
$$2HO_2 \rightarrow H_2O_2 + O_2, \quad \text{(R3)}$$
$$H_2O_2 + h\nu \rightarrow 2OH, \quad \text{(R4)}$$
$$2(OH + CO \rightarrow CO_2 + H), \quad \text{(R5)}$$
$$----------$$
$$2CO + O_2 \rightarrow 2CO_2. \quad \text{(S1)}$$

Meanwhile, although a thick and dry CO_2-rich atmosphere is unstable (Zahnle et al. 2008), in a wet and oxidized atmosphere of early Mars, CO_2 could have been stabilized by S1 (=R2+R3+R4+R5) even if the atmosphere was thick.

We estimate the H_2O_2 abundance in a warm/wet and oxidized CO_2 atmosphere by assuming that S1 is the cycle most responsible for the regeneration of CO_2 against loses due to R1. We assume that the bulk CO_2 abundance in the atmosphere is in balance between its photo-dissociation flux (R1), and twice the H_2O_2 photo-dissociation flux (R4) that produces OH for oxidizing CO. Also, it is assumed that there is no optical shielding effect for photons with wavelengths longer than the shielded wavelength, $\lambda_{\rm sh}$, but there is complete shielding for all other UV photons to H_2O_2, for simplicity. Then, the vertical column density of H_2O_2, $\Sigma_{H_2O_2}$, can be written as;

$$\Sigma_{H_2O_2} = \frac{\int_{\lambda \leq 227.5{\rm nm}} \hat{F}_\lambda d\lambda}{2\int_{\lambda_{\rm sh}}^{\lambda_{\rm th}} \hat{F}_\lambda \sigma_{{\rm diss},\lambda} d\lambda}, \quad (3)$$

where $\hat{F}_\lambda$ is solar photon flux, and $\sigma_{{\rm diss},\lambda}$ and $\lambda_{\rm th}$ are the photo-dissociation cross section and the threshold wavelength for a photon to effectively dissociate H_2O_2, respectively. Owing to the low bonding energy of H_2O_2 ($\sim$ 50 kcal/mol $\sim$ 570 nm; Bach et al. 1996), the photo-dissociation is caused not only by UV but also by visible light photons. Therefore, H_2O_2 is not completely shielded from stellar irradiation by H_2O, O_2 and CO_2 (Yung & Demore 1999). On the other hand, a developed O_3 layer may shield solar photons with wavelengths $\lesssim$ 300 nm, as displayed on Earth today. Here we use $\lambda_{\rm sh}$ = 227.5 nm and 300 nm as fiducial values of a shielded wavelength.

The dissociation cross section of H_2O_2 has been measured only for photon wavelengths in the range $\leq$ 410 nm (Kahan et al. 2012) because of the technical problem of measuring small absorption cross sections. Hence, we use $\lambda_{\rm th}$ = 410 nm as a fiducial value of the threshold wavelength. Note that, according to Kahan et al. (2012), the photolysis of H_2O_2 mainly occurs at photon wavelengths shorter than 350 nm. Therefore, inputing $\lambda_{\rm sh}$ = 227.5 nm, the measured cross section with $\lambda_{\rm th}$ = 410 nm (Lin et al. 1978; Kahan et al. 2012) and the solar spectral irradiance at 4 Ga developed by combining the observed spectrum from the Sun with those of solar-type stars at different ages (Claire et al. 2012) in Eq. (3), we find $\Sigma_{H_2O_2} \sim 8 \times 10^{17}$ cm^{-2}. When we substitute $\lambda_{\rm sh}$ = 300 nm into Eq. (3), we find $\Sigma_{H_2O_2} \sim 5 \times 10^{18}$ cm^{-2}. These values change only 10 % if the solar spectral irradiance at 3.5 Ga is used instead.

The column densities estimated here are significantly larger than the current typical value of $\sim 2 \times 10^{15}$ cm^{-2}, which corresponds to 10 ppb at 6 mbar, in the present-day Martian atmosphere. These large column densities produce optical depth over wavenumbers ν = 100–500 cm^{-1} of τ_ν = 0.003–0.6 for $\lambda_{\rm sh}$ = 227.5 nm and τ_ν = 0.02–4 for $\lambda_{\rm sh}$ = 300 nm, assuming a far-IR absorption cross section of H_2O_2, σ_{ν,H_2O_2} = 0.04–8 $\times 10^{-19}$ cm^2, which is shown in Fig. 1. Thus, if the other gases such as O_3 sufficiently can reduce the photolysis of H_2O_2, then the amount of H_2O_2 in the atmosphere would be large enough to warm the planetary surface. Note that, the column density of H_2O_2 estimated by Eq. (3) is just a typical value when S1 is the cycle most responsible for the stabilization of CO_2, while this value could be increased if the self-shielding effect was taken into account in Eq. (3). This is because we impose the restriction that only the OH produced by the photolysis of H_2O_2 is used to oxidize CO via R5, but all other reactions which produce and remove OH are ignored. Also, the other process potentially affecting the concentration of H_2O_2 is discussed in Sec 4.3.

4.2. *Condensation of H_2O_2*

It is likely that H_2O_2 in a warm and wet atmosphere of early Mars is supersaturated because the timescale for condensation is likely longer than that for photochemical production. As described later, a timescale for condensation would be much longer than that that governing the production and photo-dissociation of H_2O_2, which was shown by Nair et al. (1994), who used a photochemical model, to be of order several hours.

The condensation time can be estimated by assuming that H_2O_2 condenses as soon as it collides with conden-

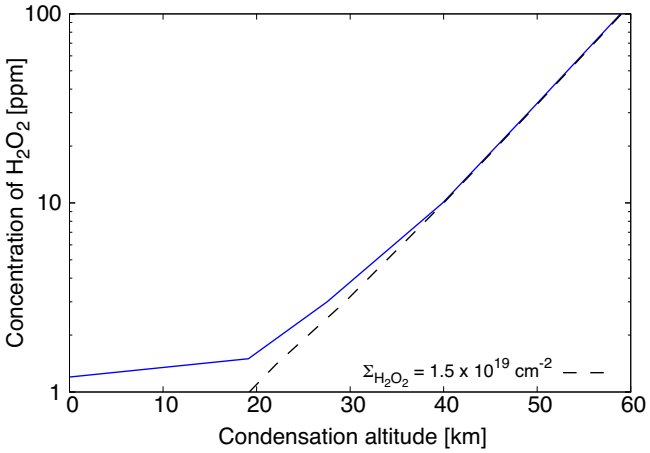


Figure 7. The concentration of H_2O_2 necessary to warm the planetary surface to 273 K in the 2–bar atmosphere as a function of the condensation altitude (see the text for the definitions of each term). The dashed line represents the column density of H_2O_2 with a constant concentration to reach $\Sigma_{H_2O_2}$ =1.5×10^{19} cm^{-2}.

sation nuclei, namely;

$$\tau_{\rm cond} = \left(4\pi r^2 N_{\rm ccn}\rho v_T\right)^{-1}, \quad (4)$$

$$\sim 50 \text{ hours} \times \quad (5)$$

$$\left(\frac{N_{\rm ccn}}{10^5 {\rm kg}^{-1}}\right)^{-1}\left(\frac{P}{0.01{\rm bar}}\right)^{-1}\left(\frac{T}{200{\rm K}}\right)^{\frac{1}{2}}\left(\frac{r}{1\mu{\rm m}}\right)^{-2},$$

where r and $N_{\rm ccn}$ are the size and concentration of the condensation nuclei, respectively, ρ is the atmospheric mass density and v_T is the thermal velocity of the gas. The timescale for condensation is longer at higher altitudes because the nuclei concentration decreases with increasing altitude. Note that, the condensation timescale is underestimated in an atmospheric region with a mean free path smaller than the size of the nuclei (i.e., a dense region) because the diffusive motion of the gas around the nuclei delays the timescale (see Lohmann et al. 2016, for the diffusive case).

Achieving sufficient warming is possible even if H_2O_2 condenses at lower altitudes due to the subsequent shorter condensation times. Fig. 7 shows the minimum H_2O_2 concentration necessary for maintaining a surface temperature of at least 273 K in a 2-bar atmosphere as a function of a condensation altitude. The condensation altitude stands for an altitude above which the H_2O_2 concentration is constant and below which all the H_2O_2 gas is virtually removed by rainout through condensation. To warm the surface environment, the required concentration of H_2O_2 needs to be about 2 ppm when the condensation altitude is no higher than about 20 km. The 2 ppm of H_2O_2 in the upper atmosphere is comparable to 1.5×10^{19} cm^{-2} which is also comparable to the H_2O_2 column density necessary to stablize the CO_2 atmosphere (Sec 4.1).

The condensation timescale will not be significantly changed if the dilution effect of H_2O_2 in an H_2O solution is taken into account. When the temperature is above $\sim$ 220 K, an H_2O–H_2O_2 solution can exist, and then the saturation vapor pressure of H_2O_2 will be lowered relative to that of pure H_2O_2 (Foley & Giguére 1951b; Manatt & Manatt 2004). However, the temperatures in the photosphere for photons with wavenumbers in the range $\geq$ 500 cm^{-1} are lower than 220 K in thick and warm atmospheres (Fig. 5). So, it is likely that aqueous solutions would be frozen in the upper atmosphere where the concentration of H_2O_2 has the greatest influence on the surface temperature. Therefore, the dilution effect of H_2O_2 in an H_2O solution would little affect the surface temperature.

4.3. *Other processes possibly affecting H_2O_2 concentration*

The atmospheric concentration of H_2O_2 can also be affected by several processes such as dissolution into water droplets, dry deposition and photochemical reactions with volcanic and reactive species (e.g., SO_2 and NO_x) (Vione et al. 2003).

Although H_2O_2 is a minor species with at most 3.5 ppb level in the Earth's atmosphere, which is mainly due to the dissolution of gaseous H_2O_2 into water droplets, where SO_2 enhances the dissolution rate (Vione et al. 2003), it might not be a minor species on early Mars during the era in which the observed Mn-oxide-rich rocks at Gale crater would have precipitated out. Since the temperatures at high altitudes in the early Martian atmosphere would be so low that H_2O would freeze, its non-dissolution into water droplets would not deplete H_2O_2. Meanwhile, at lower altitude regions, H_2O_2 would dissolve into water droplets, and precipitation would remove it.

In Earth's atmosphere, dry deposition is another removal process of atmospheric H_2O_2 at lower altitudes. Atmospheric H_2O_2 of early Mars would be vertically transported by eddy diffusion to the surface, whereby dry deposition and precipitation remove it. For the current Martian atmosphere at altitudes lower than 40 km, the scale height is $H \sim 10$ km and the vertical eddy diffusion coefficient is $K_{\rm ed} \leq 10^7 {\rm cm}^2/{\rm s}$ (Nair et al. 1994); hence the diffusion timescale is $H^2/K_{\rm ed} \geq 1$ days. Since the timescale of H_2O_2 photochemical reactions is less than a day (Nair et al. 1994; Zahnle et al. 2008), the atmospheric concentration of H_2O_2 at high altitudes is likely controlled by photochemical reactions.

The actual eddy diffusion coefficient and dry deposition timescale on early Mars would depend on turbulence/large-scale-winds and the compositions/oxidations states of the surface rocks, respectively. As such, a more detailed examination requires that photochemical calculations be done alongside those of the atmospheric thermal structure, which will be the focus of a future study.

4.4. *Oxidized early Martian environment*

An early surface environment warmed by the greenhouse effect of H_2O_2 (Sec. 4.1) is consistent with the global, highly oxidized conditions implied by the high Mn materials found on the Martian surface by the Curiosity rover in Gale crater and by the Opportunity rover in Endeavour crater (Lanza et al. 2016; Arvidson et al. 2016).

The redox state of early Martian atmosphere is likely controlled by the escape of atmospheric components into space. In the early Martian atmosphere, UV radiation from the young Sun would have enhanced hydrogen escape and effectively oxidized the atmosphere and the surface environment. In addition to hydrogen escape, the escape of atomic carbon might also have contributed to the oxidation of the early Martian atmosphere because its escape flux would not be limited by diffusion in a CO_2-rich atmosphere (N. Terada, private communications). Further studies are required to determine the redox state of the early Martian atmosphere, which could also be affected by the supply of reduced gases (e.g., CO and H_2) through volcanic degassing, oxygen escape, and oxygen uptake through weathering of the planetary surface (Zahnle et al. 2008; Wetzel et al. 2013; Batalha et al. 2015).

It is interesting to note that H_2O_2 might be able to warm a frozen planet and melt water ice. Liang et al. (2006) demonstrated that a weak hydrological cycle coupled with photochemical reactions could give rise to a sustained production of H_2O_2 during long and severe glacial intervals. Although an icy surface has a high albedo, the surface temperature can be warmed to temperatures above 273 K by a 4 and 15 ppm levels of H_2O_2 in a 2 bar atmosphere when the planetary albedo is assumed to be ≤ 0.45 and ≤ 0.5, respectively, as demonstrated by our model.

It has also been suggested that H_2O_2 deposited on the planetary surface could be stored in the ice during the time of a global snowball episode (Liang et al. 2006). If early Mars was once a snowball, and a large amount of H_2O_2 was stored in the ice, it would be released into the atmosphere upon melting caused by any mechanism, such as meteor impacts, volcanic emissions, or obliquity changes (e.g., Wordsworth 2016, references therein). The release of abundant H_2O_2 would cause not only a global oxidation event but also enhance greenhouse warming. If so, there might be geological evidence that oxidation and warming occurred simultaneously in the aftermath of a snowball Mars.

5. SUMMARY AND CONCLUSION

We investigated the possible impact of H_2O_2 as an additional greenhouse gas in a CO_2-dominant atmosphere using a one-dimensional atmospheric model. Because the timescale for condensation is longer at higher altitudes (subsection 4.2), photochemically produced H_2O_2 would likely be supersaturated in the upper atmosphere. We found that a reasonable amount of H_2O_2 in the upper atmosphere effectively cuts off the outgoing planetary radiation in the far-infrared and warms the planetary surface to a temperature hot enough to retain liquid water (Section 3).

Our results demonstrated that a warm and wet surface environment is compatible with an oxidized atmosphere on early Mars. The coexistence of liquid water and an oxidized atmosphere on early Mars has been suggested by the recent discovery of a high level of Mn in some Martian rocks (Lanza et al. 2016; Arvidson et al. 2016). Our results also indicated a key relationship between the redox state of the atmosphere and the surface temperature on early Mars, where the co-evolution of these factors may govern the surface environment over geological time scales. This important phenomenon will be the subject of future work, which will aim to understand the surface environment under an oxidized atmosphere on early Mars.

ACKNOWLEDGMENTS

We thank Ramses Ramirez for sharing their albedo data of CO_2 atmospheres with us. This work was supported by MEXT/JSPS KAKENHI Grants Numbers 17H06457, 18K03719, and 19H01947 and by NINS Astrobiology Center Project Grant Numbers AB311025.

REFERENCES

Andrews, D. G. 2000, An Introduction to Atmospheric Physics, 240

Arvidson, R. E., Squyres, S. W., Morris, R. V., et al. 2016, American Mineralogist, 101, 1389, doi: 10.2138/am-2016-5599

Bach, R. D., Ayala, P. Y., & Schlegel, H. B. 1996, Journal of the American Chemical Society, 118, 12758, doi: 10.1021/ja961838i

Baranov, Y. I., Lafferty, W. J., & Fraser, G. T. 2004, Journal of Molecular Spectroscopy, 228, 432, doi: 10.1016/j.jms.2004.04.010

Batalha, N., Domagal-Goldman, S. D., Ramirez, R., & Kasting, J. F. 2015, Icarus, 258, 337, doi: 10.1016/j.icarus.2015.06.016

Claire, M. W., Sheets, J., Cohen, M., et al. 2012, ApJ, 757, 95, doi: 10.1088/0004-637X/757/1/95

Encrenaz, T., Bézard, B., Greathouse, T. K., et al. 2004, Icarus, 170, 424, doi: 10.1016/j.icarus.2004.05.008

Foley, W. T., & Giguére, P. A. 1951a, Canadian Journal of Chemistry, 29, 895, doi: 10.1139/v51-104

—. 1951b, Canadian Journal of Chemistry, 29, 123, doi: 10.1139/v51-016

Forget, F., & Pierrehumbert, R. T. 1997, Science, 278, 1273, doi: 10.1126/science.278.5341.1273

Gao, P., Hu, R., Robinson, T. D., Li, C., & Yung, Y. L. 2015, ApJ, 806, 249, doi: 10.1088/0004-637X/806/2/249

Gruszka, M., & Borysow, A. 1997, Icarus, 129, 172, doi: 10.1006/icar.1997.5773

Johnson, S. S., Mischna, M. A., Grove, T. L., & Zuber, M. T. 2008, Journal of Geophysical Research (Planets), 113, E08005, doi: 10.1029/2007JE002962

Kahan, T. F., Washenfelder, R. A., Vaida, V., & Brown, S. S. 2012, Journal of Physical Chemistry A, 116, 5941, doi: 10.1021/jp2104616

Kasting, J. F. 1988, Icarus, 74, 472, doi: 10.1016/0019-1035(88)90116-9

—. 1991, Icarus, 94, 1, doi: 10.1016/0019-1035(91)90137-I

Kasting, J. F., Brown, L. L., Acord, J. M., & Pollack, J. B. 1992, in Martian Surface and Atmosphere Through Time, ed. R. M. Haberle & B. M. Jakosky, 84

Kasting, J. F., Pollack, J. B., & Ackerman, T. P. 1984, Icarus, 57, 335, doi: 10.1016/0019-1035(84)90122-2

Keller-Rudek, H., Moortgat, G. K., Sander, R., & Sörensen, R. 2013, Earth System Science Data, 5, 365, doi: 10.5194/essd-5-365-2013

Kopparapu, R. K., Ramirez, R., Kasting, J. F., et al. 2013, ApJ, 765, 131, doi: 10.1088/0004-637X/765/2/131

Lanza, N. L., Wiens, R. C., Arvidson, R. E., et al. 2016, Geophys. Res. Lett., 43, 7398, doi: 10.1002/2016GL069109

Liang, M.-C., Hartman, H., Kopp, R. E., Kirschvink, J. L., & Yung, Y. L. 2006, Proceedings of the National Academy of Science, 103, 18896, doi: 10.1073/pnas.0608839103

Lin, C. L., Rohatgi, N. K., & Demore, W. B. 1978, Geophys. Res. Lett., 5, 113, doi: 10.1029/GL005i002p00113

Lohmann, U., Lüönd, F., & Mahrt, F. 2016, An Introduction to Clouds: From the Microscale to Climate (Cambridge University Press), doi: 10.1017/CBO9781139087513

Manatt, S. L., & Manatt, M. R. R. 2004, Chemistry – A European Journal, 10, 6540, doi: 10.1002/chem.200400104

Maroulis, G. 1992, The Journal of Chemical Physics, 96, 6048, doi: 10.1063/1.462646

Meadows, V. S., & Crisp, D. 1996, J. Geophys. Res., 101, 4595, doi: 10.1029/95JE03567

Nair, H., Allen, M., Anbar, A. D., Yung, Y. L., & Clancy, R. T. 1994, Icarus, 111, 124, doi: 10.1006/icar.1994.1137

Noda, N., Imamura, S., Sekine, Y., et al. 2019, Journal of Geophysical Research (Planets), 124, 1282, doi: 10.1029/2018JE005892

Parkinson, T. D., & Hunten, D. M. 1972, Journal of Atmospheric Sciences, 29, 1380, doi: 10.1175/1520-0469(1972)029<1380:SAAOOO>2.0.CO;2

Perrin, M. Y., & Hartmann, J. M. 1989, JQSRT, 42, 311, doi: 10.1016/0022-4073(89)90077-0

Postawko, S. E., & Kuhn, W. R. 1986, J. Geophys. Res., 91, D431, doi: 10.1029/JB091iB04p0D431

Press, W. H., Teukolsky, S. a., Vetterling, W. T., & Flannery, B. P. 1996, Numerical Recipes in Fortran 77: the Art of Scientific Computing. Second Edition, Vol. 1

Ramirez, R. M. 2017, Icarus, 297, 71, doi: 10.1016/j.icarus.2017.06.025

Ramirez, R. M., & Craddock, R. A. 2018, Nature Geoscience, 11, 230, doi: 10.1038/s41561-018-0093-9

Ramirez, R. M., Kopparapu, R., Zugger, M. E., et al. 2014, Nature Geoscience, 7, 59, doi: 10.1038/ngeo2000

Rothman, L. S., Gordon, I. E., Babikov, Y., et al. 2013, JQSRT, 130, 4, doi: 10.1016/j.jqsrt.2013.07.002

Sagan, C., & Mullen, G. 1972, Science, 177, 52, doi: 10.1126/science.177.4043.52

Schaefer, L., Wordsworth, R. D., Berta-Thompson, Z., & Sasselov, D. 2016, ApJ, 829, 63, doi: 10.3847/0004-637X/829/2/63

Tennyson, J., & Yurchenko, S. N. 2018, Atoms, 6, doi: 10.3390/atoms6020026

Tian, F., Claire, M. W., Haqq-Misra, J. D., et al. 2010, Earth and Planetary Science Letters, 295, 412, doi: 10.1016/j.epsl.2010.04.016

Vione, D., Maurino, V., Minero, C., & Pelizzetti, E. 2003, Annali di chimica, 93, 477

Wetzel, D. T., Rutherford, M. J., Jacobsen, S. D., Hauri, E. H., & Saal, A. E. 2013, Proceedings of the National Academy of Science, 110, 8010, doi: 10.1073/pnas.1219266110

Wordsworth, R., Forget, F., Millour, E., et al. 2013, Icarus, 222, 1, doi: 10.1016/j.icarus.2012.09.036

Wordsworth, R., Kalugina, Y., Lokshtanov, S., et al. 2017, Geophys. Res. Lett., 44, 665, doi: 10.1002/2016GL071766

Wordsworth, R. D. 2016, Annual Review of Earth and Planetary Sciences, 44, 381, doi: 10.1146/annurev-earth-060115-012355

Yung, Y. L., & Demore, W. B., eds. 1999, Photochemistry of planetary atmospheres: Oxford University Press, QB603.A85 Y86 1999, doi: 10.1021/ja9957938

Yurchenko, S. N., Al-Refaie, A. F., & Tennyson, J. 2018, A&A, 614, A131, doi: 10.1051/0004-6361/201732531

Zahnle, K., Haberle, R. M., Catling, D. C., & Kasting, J. F. 2008, Journal of Geophysical Research (Planets), 113, E11004, doi: 10.1029/2008JE003160